2014

Extracting continuum-like deformation and stress from molecular dynamics simulations

Lili Zhang
University of Oxford

John Jasa
University of Nebraska-Lincoln

George Gazonas
Aberdeen Proving Ground

Antoine Jerusalem
University of Oxford

Mehrdad Negahban
University of Nebraska-Lincoln, mnegahban1@unl.edu

Available online at www.sciencedirect.com
ScienceDirect
Comput. Methods Appl. Mech. Engrg. 283 (2015) 1010–1031
Computer methods in applied mechanics and engineering
www.elsevier.com/locate/cma

Extracting continuum-like deformation and stress from molecular dynamics simulations

Lili Zhang[c], John Jasa[a], George Gazonas[b], Antoine Jérusalem[c], Mehrdad Negahban[a,*]

[a] *Department of Mechanical and Materials Engineering, University of Nebraska-Lincoln, Lincoln, NE 68588-0526, USA*
[b] *U.S. Army Research Laboratory, Aberdeen Proving Ground, MD 21005, USA*
[c] *Department of Engineering Science, University of Oxford, Oxford, OX1 3PJ, UK*

Received 18 June 2014; received in revised form 26 September 2014; accepted 16 October 2014
Available online 25 October 2014

Abstract

We present methods that use results from molecular dynamics (MD) simulations to construct continuum parameters, such as deformation gradient and Cauchy stress, from all or any part of an MD system. These parameters are based on the idea of minimizing the difference between MD measures for deformation and traction and their continuum counterparts. The procedures should be applicable to non-equilibrium and inhomogeneous systems, and to any part of a system, such as a polymer chain. The resulting procedures provide methods to obtain first and higher order deformation gradients associated with any subset of the MD system, and associated expressions for the Cauchy and nominal stresses. As these procedures are independent of the type of interactions, they can be used to study any MD simulation in a manner consistent with continuum mechanics and to extract information exploitable at the continuum scale to help construct continuum-level constitutive models.

Keywords: Molecular dynamics; Multi-scale; Deformation; Deformation gradients; Stress; Minimization

1. Introduction

In this article we define continuum-like deformation and stress measures for a system of interacting particles. This is motivated by the need to connect results from discrete atomistic simulations to analysis at the continuum scale. In particular, the ease of conducting molecular dynamics (MD) simulations now allows us to look more closely at how materials behave at the atomic level, yet the size of the systems considered and time scale on which one can do this are limited. One method to remove these limitations is to connect the atomic simulations to how we understand response and how we analyze problems at the continuum level.

MD is a very simple and powerful tool that has been used to study the behavior of all kinds of microstructures by essentially solving Newton's equations for trajectories of a system of interacting particles. One application is in the characterization of macroscopic properties based on using MD simulations and multi-scaling to obtain the continuum

* Correspondence to: W311 NH, University of Nebraska-Lincoln, Lincoln, NE 68588-0526, USA. Tel.: +1 402 472 2397; fax: +1 402 472 1465.
E-mail address: mnegahban@unl.edu (M. Negahban).

http://dx.doi.org/10.1016/j.cma.2014.10.018
0045-7825/

response based on simulated molecular-scale mechanisms. This has initiated the study of how to define continuum-level parameters based on knowledge of the atomic MD simulations and has resulted in a number of definitions for calculating variables, such as deformation gradient and stress, based on an MD simulation. The most influential of these have been the expression developed for virial stress in 1870 by Clausius [1] for systems in thermodynamic equilibrium, the Irving and Kirkwood [2] procedure to calculate stress in 1950, and its generalization by Hardy [3] in 1982 for inhomogeneous systems and for systems out-of-equilibrium. Most of these methods have found their way into standard calculations and are now included in texts of statistical mechanics and MD simulation, such as the recent texts by Tuckerman [4] and by Tadmor [5].

With the increase in computational power enjoyed in the past three decades and the development of readily available MD simulation programs, such as LAMMPS [6,7] from Sandia, NAMD [8] and VMD [9] from the University of Illinois, CHARMM [10,11] from Harvard and Materials Studio [12] from Accelrys, the use of MD has increased substantially and a new interest has developed to find new ways to use this tool. This interest has also resulted in a number of works that have revisited the original works [1–3] to find new ways to extract continuum parameters from MD simulations [13–22].

In building a continuum measure of deformation, we use the ideas of Gullett et al. [23] and its extension by Zimmerman et al. [24]. Gullett et al. [23] propose a kinematical algorithm for the construction of an atom-centered deformation gradient tensor from atomistic simulation data based on a least-square minimization between the continuum mapping and the molecular motion. In this case, the discrete incremental form of the deformation gradient emerges from a weighted least-square minimization that includes the distances from the specific atom in question. Zimmerman et al. [24] extend this definition to higher gradients and thus introduce both first and second gradients of deformation at the atom.

We use this same idea to define continuum deformations that are constructed from MD simulations, but that are associated with a system of particles, as opposed to a single atom. This allows, for example in a macromolecular system, to discuss the deformation gradient associated with a single polymer chain of the system. These expressions for deformation and its gradients are very similar to those proposed in Refs. [23,24], simply extended to systems as opposed to a single atom, and centered on the system's average location, such as its centroid or center of mass.

We adopt a similar method for calculating stress. In particular, as in Refs. [23,24], we base the calculation on minimizing the difference between the associated molecular and continuum counterparts. More specifically, we construct the continuum-level stress by minimizing the difference between the continuum and MD definitions of traction. As will be shown, these procedures produce continuum measures for nominal and Cauchy stress that differ from what has been proposed by others.

As can be deduced from the following review of the work on describing continuum-like measures of deformation and stress for atomic systems, the current state of knowledge does not include clear measures of deformation and stress associated with arbitrary selected parts of an MD system. The proposed measures of deformation (and its gradients) and stress can do this. For example, one can select a single polymer strand that is entangled in other strands and express measures of its deformation and stress.

1.1. Descriptions of macroscopic deformation based on microscopic simulation

Mott et al. [25] in 1992 proposed a definition of the local atomic strain increments in three dimensions and an algorithm for computing them. This was done for an arbitrary arrangement of atoms tessellated into Delaunay tetrahedra by identifying interstices, and Voronoi polyhedra by identifying atomic domains. The deformation gradient increment tensor for interstitial space was then obtained from the displacement increments of the corner atoms of the Delaunay tetrahedra. The atomic site strain increment tensor was obtained by finding the intersection of the Delaunay tetrahedra with the Voronoi polyhedra, accumulating the individual deformation gradient contributions of the intersected Delaunay tetrahedra into the Voronoi polyhedra.

Costanzo et al. [26] reviewed the continuum notions of effective deformation gradient and effective stress for homogenization problems with large deformations. The focus of their work was on the role played by boundary conditions in defining a meaningful space average of deformation and stress, and establishing a connection between the idea of effective stress from micro-mechanics and that based on the virial theorem.

Gullett et al. [23] proposed a kinematical algorithm for the construction of an atom-centered deformation gradient tensor from atomistic simulation data based on a least-square minimization of the continuum mapping and the

molecular motion. Local strain tensors such as the Almansi and Green strain tensors suitable for use in large deformation simulations were computed directly from a discrete form of the atom-based deformation gradient. The discrete incremental form of the deformation gradient emerged from a weighted least-square-minimization that included a length scale relating the distance from the atom in question. This region defined the nonlocal domain of the strain at the that atom level. Zimmerman et al. [24] extended this definition to higher gradients and thus introduced both first and second gradients of deformation at the atom level. These expressions were necessary for linking atomistic simulation results with advanced continuum mechanics theories such as strain gradient plasticity, thereby enabling fundamental, atomic-scale information to contribute to the formulation and parameterization of such theories.

Stukowski et al. [27] developed a practical technique to perform the multiplicative decomposition of the deformation field into elastic and plastic parts for the case of crystalline materials. The described computational analysis method can be used to quantify plastic deformation in a material due to crystal slip-based mechanisms in MD and molecular statics (MS) simulations. The authors built up on an idea first published by Mott et al. [25], which yielded a continuum tensor field from the displacements of atoms using a Delaunay tessellation of space. Tucker et al. [28] employed atomistic simulations to investigate the deformation of nano-crystalline copper and the associated strain accommodation mechanisms as a function of grain size. Volume-averaged kinematic metrics based on continuum mechanics theory were formulated to analyze the results of MD simulations. As a first step toward the development of physics-based models of deformation in the presence of a crack, Saitoh et al. [29] proposed a simple method to analyze atomistic strain in MD simulation. This method, called atomic strain measure (ASM), was based on the Green–Lagrange strain measure of continuum mechanics. The ASM was formulated for use in atomic systems with some adequate assumptions. In their formulation, pairwise interatomic vectors of finite length were approximately substituted for infinitesimal continuum line segments between material points. The obtained expression of ASM was very simple and easy to use. Zhang et al. [22] proposed a comprehensive approach based on MD simulations of a crystalline material with an embedded crack. Effective characterization methods like common neighbor analysis, dislocation extraction algorithm and atomic-scale deformation gradient analysis followed by quantification were able to delineate the crack length/opening, dislocation structure and micro-twins at a high resolution. Ultimately the authors developed a simple mechanistic model of deformation, which associated dislocation density evolution with the stress–strain response in a crystalline material in the presence of a crack.

1.2. Descriptions of macroscopic stress based on microscopic simulation

Irving and Kirkwood [2] derived the equations of hydrodynamic continuity, motion, and energy transport by means of classical statistical mechanics. The authors obtained the stress tensor and heat current density in terms of molecular variables. Continuing the work of Irving and Kirkwood, Noll [30] proved two lemmas that allowed him to avoid the use of the Dirac delta distribution, and thus resulted in a closed-form expression for the stress tensor without the need for a series expansion. The procedure introduced by Irving and Kirkwood and extended by Noll was later referred to as the Irving–Kirkwood–Noll procedure. Hardy [3] gave the formulas that relate the mass, momentum, and energy densities and the momentum and heat fluxes to the masses, positions, and velocities of the individual particles making up a system. The formulas of Hardy were similar to those of Irving and Kirkwood, but had forms that were easily implemented in MD simulations. Corrections to the virial formula for the pressure and to the related formulas for the stress tensor and heat flux were obtained.

Cheung et al. [31] considered the determination of the local stress distribution in a system with atomic-level inhomogeneities. Atomistic simulation results were presented to show that for a relaxed crystal with a planar free surface, the normal stress on each atomic plane parallel to the surface, when calculated according to the mechanical definition, vanished uniformly as expected, whereas if the virial expression were applied, the resulting stress distribution showed unphysical oscillations in the surface region.

Machová [32] examined different definitions of the local atomic stress at zero temperature for homogeneous and inhomogeneous strain across an interface. It was shown that if inhomogeneous straining occured within the range of interatomic interaction, then the interplanar concept (based on force balance) described better the local stress in comparison with a definition of the volume stress derived from the energy density around an atom.

Zhou et al. [33] defined an equivalent continuum for dynamically deforming atomistic particle systems treated with concepts of MD. The discrete particle systems considered exhibited micro-polar interatomic interactions which involved both central interatomic forces and interatomic moments. The equivalence of the continuum to discrete

atomic systems included, firstly, preservation of linear and angular momenta, secondly, conservation of internal, external and inertial rates of work and, thirdly, conservation of mass. Zhou [34] demonstrated that, contrary to the belief of some in the physics/mechanics/materials communities, the virial stress was not the Cauchy stress or any other form of mechanical stress as it did not measure internal mechanical force in any sense. The most important conclusion of the paper was that the virial stress had a geometric interpretation without any physical significance. Specifically, the paper showed that the virial stress measured the rate of momentum change in space.

Shen et al. [35] defined an atomistic-level stress tensor with physical clarity, based on the Smoothed Particle Hydrodynamics (SPH) method. This stress tensor rigorously satisfied the conservation of linear momentum, and was appropriate for both homogeneous and inhomogeneous deformations. An equivalent continuum was also defined for the MD system, based on the developed definition of atomistic stress and in conjunction with the SPH technique.

Zimmerman et al. [36] compared an expression for continuum mechanical stress in atomistic systems derived by Hardy with the expression for atomic stress taken from the virial theorem. Hardy's stress expression was evaluated at a fixed spatial point and used a localization function to dictate how nearby atoms contribute to the stress at that point; thereby performing a local spatial averaging. The authors presented the results on extending Hardy's spatial averaging technique to include temporal averaging for finite temperature systems. Costanzo et al. [37] reviewed the continuum notions of average mechanical properties such as stress and strain and the meaning of such notions when MD was used to compute them. The focus of their work was a discussion of how boundary conditions were actually enforced in MD and what corresponding notion of averages was therefore appropriate.

Chen and Fish [13] derived a continuum stress measure from MD equations using a Generalized Mathematical Homogenization (GMH) theory. GMH consisted in solving a coupled fine-scale (atomistic unit cell) problem and a coarse-scale (continuum) problem. The continuum stress derived was compared to various versions of the virial stress formula.

Murdoch [14] compared different definitions and derivations of the stress tensor in terms of atoms/molecules, modeled as interacting point masses. The author elucidated assumptions inherent to different approaches, and clarified the associated physical interpretations of stress. Following a critical analysis and extension of the virial approach, a method of spatial atomistic averaging (at any prescribed length scale) was presented and a balance of linear momentum was derived. Subramaniyan et al. [15] reviewed the equivalence of the virial stress and Cauchy stress using both theoretical arguments and numerical simulations. Using thermo-elasticity problems as examples, the authors numerically demonstrated that the virial stress was equivalent to the continuum Cauchy stress. It was shown that neglecting the velocity terms in the definition of virial stress as many authors had recently suggested can cause significant errors in interpreting MD simulation results at elevated temperatures. Webb et al. [16] reviewed the calculation of stress, heat flux, and temperature in atomic scale numerical simulations such as the MD method.

Liu et al. [38] discussed how to objectively compute the equivalent atomic stress and connect it to the Cauchy stress. The authors proposed the fundamental Lagrangian atomic stress by strictly following the classical definition of the Cauchy stress for a continuum medium. Xu et al. [17] used three typical atomistic simulation examples to validate various existing stress definitions. The authors found that the Lagrangian cross-section stress and virial stress were validated by these examples. An instantaneous Lagrangian atomic stress definition was also proposed for dynamical problems.

Admal et al. [18] set up a unified framework in which all existing definitions for the Cauchy stress can be derived, thus establishing the connections between them. The framework was based on the non-equilibrium statistical mechanics procedure introduced by Irving, Kirkwood [2] and Noll [30], followed by spatial averaging. Connections between this approach and the direct spatial averaging approach of Murdoch [14] and Hardy [3] were discussed and the Murdoch–Hardy procedure was systematized.

Maranganti et al. [19] provided a unified setting that connected continuum, empirical MD and quantum mechanical stress concepts. The essential tool was provided by Murdoch's formalism [14] aimed at reaching a spatially varying stress field in a discrete setting. Analogous to MD, Hardy and Noll stress-like operators can represent the microscopic stress measures in quantum mechanics.

Batra et al. [39] used MS simulations to study axial tension/compression and simple axial tension/compression of prismatic gold nano-rods of square cross section with the tight-binding potential with the goal of delineating stress distributions in the specimen. For triaxial deformations of the specimen, the authors have also compared Cauchy stresses computed with Hardy's method from results of the MS simulations with those found by assuming that the

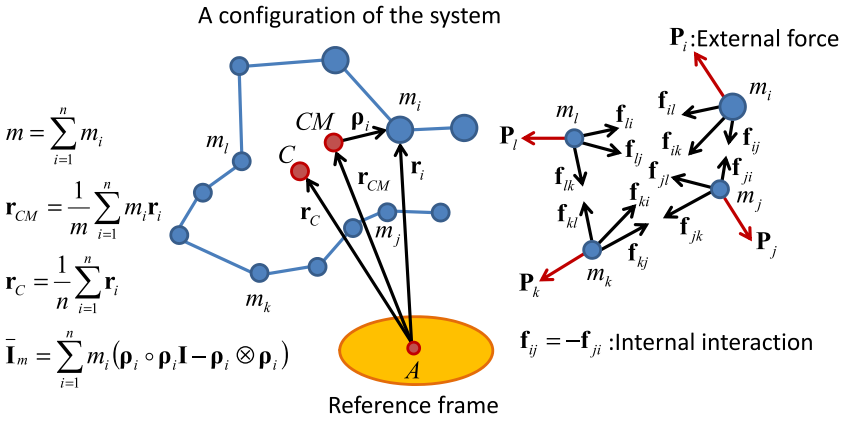

Fig. 1. A configuration of the molecular system and typical characteristics.

material was hyperelastic, and whose strain energy was derived from the tight-binding potential and the Cauchy–Born rule.

Zimmerman et al. [40] presented a material frame formulation analogous to the spatial frame formulation developed by Hardy [3], whereby expressions for continuum mechanical variables such as stress and heat flux were derived from atomic-scale quantities intrinsic to molecular simulations. The authors derived expressions for the first Piola–Kirchhoff stress tensor and the material frame heat flux vector directly from the momentum and energy balances using localization functions in a reference configuration.

Yang et al. [20] extended Hardy's formulas by systematically incorporating both spatial and temporal averaging into the expression of continuum quantities. The derivation followed the Irving–Kirkwood formalism, and the average quantities still satisfied conservation laws in continuum mechanics.

2. Preliminary information and notation

In MD simulations, sets of atoms, as shown in Fig. 1, interact through forces defined by a set of interaction potentials. In the simulation, the motion of these atoms is followed and the forces are updated based on the current locations of the individual atoms. As a result, the output of the MD simulation is the history of atomic positions, defining the trajectories of the atoms in the simulation.

A subscript index is used to denote the particle so that m_i and $\mathbf{r}_i$ are, respectively, the mass and position of particle i. The symbol Ω denotes the set of all indices for the system so that, for example, the total mass m and the center of mass $\mathbf{r}_{CM}$ for the system can be written, respectively, as

$$m=\sum_{i\in\Omega} m_i, \tag{1}$$

$$\mathbf{r}_{CM}=\frac{1}{m}\sum_{i\in\Omega} m_i\mathbf{r}_i. \tag{2}$$

The symbol $\boldsymbol{\rho}_i$ denotes the relative position of m_i to the center of mass of the selected set so that

$$\mathbf{r}_i=\mathbf{r}_{CM}+\boldsymbol{\rho}_i. \tag{3}$$

As shown in Fig. 1, both interaction forces between the particles of the system and forces applied from outside of the system are considered. Let $\mathbf{P}_i$ denote the resultant external force applied on particle i, and $\mathbf{f}_{ij}$ denote the force of interaction exerted by particle j on particle i. As expected, $\mathbf{P}_i$ will include any existing body forces and all forces of interaction between particles inside and outside the selected system. Only the interaction between particles inside the selected system is represented in $\mathbf{f}_{ij}$. From Newton's third law one has

$$\mathbf{f}_{ij}=-\mathbf{f}_{ji}. \tag{4}$$

Note that one could define other weighted centers for the system using a general averaging method given as

$$\mathbf{r}_w = \frac{1}{w}\sum_{i\in\Omega} w_i \mathbf{r}_i, \tag{5}$$

where w_i is the weight used for particle i and $w = \sum_{i\in\Omega} w_i$ is the sum of these weights. The obvious weights are unit or particle masses, which, respectively, give us the centroid and the center of mass.

The virial stress $\boldsymbol{\sigma}$ defined by Clausius [1], and given in Ref. [16], can be written as

$$\boldsymbol{\sigma} = \frac{1}{V}\sum_{i\in\Omega}\left[\frac{1}{2}\sum_{j\neq i\in\Omega}(\mathbf{r}_i - \mathbf{r}_j)\otimes\mathbf{f}_{ij} - m_i\mathbf{v}_i\otimes\mathbf{v}_i\right], \tag{6}$$

where V is the system representative volume, and $\mathbf{v}_i$ is the velocity of particle i, and where it is assumed that the system momentum is zero. The Irving and Kirkwood [2] procedure and the Hardy [3] assumption result in a Cauchy stress that is given by

$$\boldsymbol{\sigma}(\mathbf{x},t) = -\sum_{i\in\Omega}\left[\frac{1}{2}\sum_{j\neq i\in\Omega}(\mathbf{r}_i - \mathbf{r}_j)\otimes\mathbf{f}_{ij}B_{ij}(\mathbf{x}) + m_i(\mathbf{v}_i - \mathbf{v})\otimes(\mathbf{v}_i - \mathbf{v})\psi(\mathbf{r}_i - \mathbf{x})\right], \tag{7}$$

where $\mathbf{v}$ is the equivalent continuum velocity at the point $\mathbf{x}$, $\psi(\mathbf{r}_i - \mathbf{x})$ is a localization function related to the position of the particle relative to the point of evaluation of the stress, and $B_{ij}(\mathbf{x})$ is the bond function between atoms given as

$$B_{ij}(\mathbf{x}) = \int_0^1 \psi[\mathbf{r}_j + \lambda(\mathbf{r}_i - \mathbf{r}_j) - \mathbf{x}]d\lambda. \tag{8}$$

Let ρ and $\mathbf{p}$ denote, respectively, the equivalent continuum density and linear momentum at point $\mathbf{x}$ and given by

$$\rho(\mathbf{x},t) = \sum_{i\in\Omega} m_i\psi[\mathbf{r}_i(t) - \mathbf{x}], \tag{9}$$

$$\mathbf{p}(\mathbf{x},t) = \sum_{i\in\Omega} m_i\mathbf{v}_i(t)\psi[\mathbf{r}_i(t) - \mathbf{x}]. \tag{10}$$

The Hardy stress reduces to the Irving and Kirkwood [2] stress for a Dirac delta localization function. This process also provides a velocity gradient $\mathbf{L}$ given by

$$\begin{aligned}\mathbf{L} &= \operatorname{grad}(\mathbf{v}) = \operatorname{grad}\left(\frac{\mathbf{p}}{\rho}\right)\\ &= \frac{1}{\rho}\operatorname{grad}(\mathbf{p}) - \frac{1}{\rho^2}\mathbf{p}\otimes\operatorname{grad}(\rho)\\ &= \frac{1}{\rho}\sum_{i\in\Omega} m_i\mathbf{v}_i\otimes\operatorname{grad}[\psi(\mathbf{r}_i - \mathbf{x})] - \frac{1}{\rho^2}\mathbf{p}\otimes\sum_{i\in\Omega} m_i\operatorname{grad}[\psi(\mathbf{r}_i - \mathbf{x})].\end{aligned} \tag{11}$$

3. Continuum measures from MD calculations

3.1. Deformation measures

The goal is to understand and define values of continuum measures based on results from MD simulations. To make this transition from molecular motion to continuum concepts, we follow a development similar to that proposed in Gullett et al. [23] and Zimmerman et al. [24]. It is assumed that a motion function, similar to that in continuum mechanics, exists that gives points in the current configuration in terms of their locations in a reference configuration. This motion function is written in the traditional manner as $\mathbf{x}(\mathbf{X},t)$, where $\mathbf{x}$ is the current location at time t of the

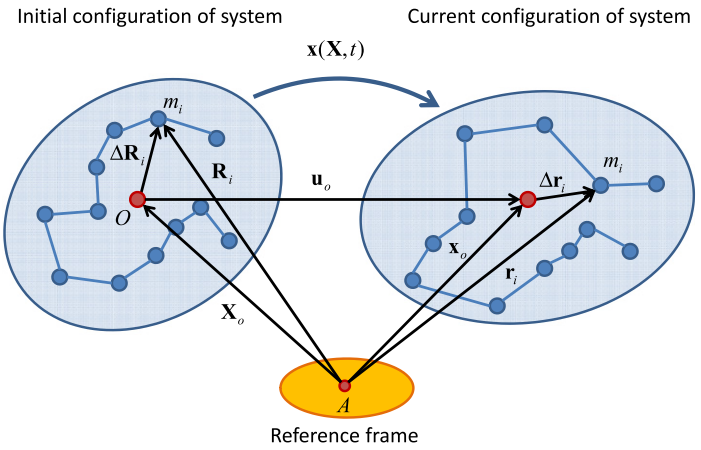

Fig. 2. Reference and current configurations of the MD system and an overlaid continuum.

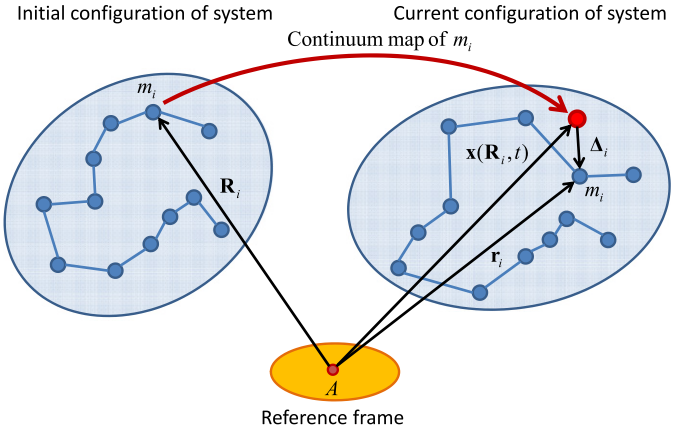

Fig. 3. Error between the continuum map and the particle motion.

particle that is at location $\mathbf{X}$ in the reference configuration, see Fig. 2. This mapping allows us to construct a Taylor series expansion at any point $\mathbf{X}_o$ as

$$\mathbf{x}(\mathbf{X},t) = \mathbf{x}(\mathbf{X}_o,t) + \mathbf{F}(t)(\mathbf{X}-\mathbf{X}_o) + \frac{1}{2}\mathbf{F}^{(2)}(t) : [(\mathbf{X}-\mathbf{X}_o)\otimes(\mathbf{X}-\mathbf{X}_o)] + \frac{1}{3!}\mathbf{F}^{(3)}(t)\vdots[(\mathbf{X}-\mathbf{X}_o)\otimes(\mathbf{X}-\mathbf{X}_o)\otimes(\mathbf{X}-\mathbf{X}_o)] + \cdots, \tag{12}$$

where $\mathbf{F}(t)$ is the first spatial gradient with respect to $\mathbf{X}$ of the motion evaluated at $\mathbf{X}_o$, $\mathbf{F}^{(n)}(t)$ is the n^{th} spatial gradient at $\mathbf{X}_o$. Without loss of generality, time is left out from the notation, essentially only looking at two configurations, so that

$$\mathbf{x} = \mathbf{x}_o + \mathbf{F}\Delta\mathbf{X} + \frac{1}{2}\mathbf{F}^{(2)} : (\Delta\mathbf{X}\otimes\Delta\mathbf{X}) + \frac{1}{3!}\mathbf{F}^{(3)}\vdots(\Delta\mathbf{X}\otimes\Delta\mathbf{X}\otimes\Delta\mathbf{X}) + \cdots, \tag{13}$$

where $\mathbf{x}_o = \mathbf{x}(\mathbf{X}_o,t)$ and $\Delta\mathbf{X} = \mathbf{X}-\mathbf{X}_o$. Our task is to somehow match the motion from the MD simulation with that from the continuum motion function by evaluating appropriate expressions for the terms in this expansion. In particular, as in Refs. [23,24] a least-square minimization process is used to minimize the difference between the continuum motion and the motions seen in the corresponding MD simulation. As is common in data regression, the current position function is written as $\mathbf{x}^{\dagger}(\mathbf{X},t;\mathbf{X}_o,\mathbf{x}_o,\mathbf{F},\mathbf{F}^{(2)},\ldots,\mathbf{F}^{(m)})$ for a truncation after the m^{th} gradient.

Reference and current configurations can be defined for the MD system in a similar manner as is defined for their continuum counterparts, see Fig. 3. Likewise, particle i in the reference configuration is at $\mathbf{R}_i$ and in the current

configuration is at $\mathbf{r}_i(t)$. As might be expected, by introducing the reference location of any particle into the continuum motion function one obtains a current location that is not exactly where the actual particle is. Let us denote this difference for particle i as $\boldsymbol{\Delta}_i$ so that

$$\mathbf{r}_i(t) = \mathbf{x}(\mathbf{R}_i, t) + \boldsymbol{\Delta}_i(t). \tag{14}$$

The total error for the system can be evaluated by introducing an error function that sums the error of all the individual particles. Let the overall system error $R(t)$ be defined as

$$R(t) = \frac{1}{2}\sum_{i\in\Omega} w_i\, \boldsymbol{\Delta}_i(t) \circ \boldsymbol{\Delta}_i(t), \tag{15}$$

where w_i is a weighting factor that, for example, can be taken as unity for a geometric error measure, or as the particle mass for an inertia weighted error function. The former is an example associated, for example, with the centroid, as opposed to the latter that is associated with the center of mass. Note that for a simple regression, the function describing the continuum motion would be defined by a set of scalar parameters c_j, parameters that one selects to minimize the global error. As is common in data regression, the motion function described by m parameters would be expressed by the notation $\mathbf{x}(\mathbf{X}, t; c_1(t), \ldots, c_m(t))$ and the optimal fit would be the one for which the variation in R is zero for all possible variations of the parameters c_j. This corresponds to finding the stationary point of the overall system error. The variation in R is written as

$$\delta R(t) = \sum_{j=1}^{m} \frac{\partial R}{\partial c_j}\delta c_j, \tag{16}$$

where δc_j is the variation in c_j. At the stationary point the variation in R should be equal to zero for all δc_j, which requires that $\frac{\partial R}{\partial c_j} = 0$ for all parameters c_j. This, in turn, results in

$$\sum_{i\in\Omega} w_i\, \boldsymbol{\Delta}_i(t) \circ \frac{\partial \boldsymbol{\Delta}_i(t)}{\partial c_j} = 0, \tag{17}$$

which is then solved for the unknown parameters. In our case, the parameters are not scalars, but the process is similar. We wish to model the motion by the truncated Taylor series expansion of Eq. (12) that can be written as $\mathbf{x}(\mathbf{X}, t) = \mathbf{x}^{\dagger}(\mathbf{X}, t; \mathbf{X}_o, \mathbf{x}_o, \mathbf{F}, \mathbf{F}^{(2)}, \ldots, \mathbf{F}^{(m)})$. Similar to regular regression, a system of equations is obtained to solve for $\mathbf{x}_o, \mathbf{F}, \mathbf{F}^{(2)}, \ldots,$ and $\mathbf{F}^{(m)}$ that has the form

$$\sum_{i\in\Omega} w_i \left\{\mathbf{r}_i - \mathbf{x}_o - \mathbf{F}\Delta\mathbf{R}_i - \frac{1}{2}\mathbf{F}^{(2)} : (\Delta\mathbf{R}_i \otimes \Delta\mathbf{R}_i) - \cdots\right\} = \mathbf{0}, \tag{18}$$

$$\sum_{i\in\Omega} w_i \left\{\mathbf{r}_i - \mathbf{x}_o - \mathbf{F}\Delta\mathbf{R}_i - \frac{1}{2}\mathbf{F}^{(2)} : (\Delta\mathbf{R}_i \otimes \Delta\mathbf{R}_i) - \cdots\right\} \otimes \Delta\mathbf{R}_i = \mathbf{0}, \tag{19}$$

$$\sum_{i\in\Omega} w_i \left\{\mathbf{r}_i - \mathbf{x}_o - \mathbf{F}\Delta\mathbf{R}_i - \frac{1}{2}\mathbf{F}^{(2)} : (\Delta\mathbf{R}_i \otimes \Delta\mathbf{R}_i) - \cdots\right\} \otimes \Delta\mathbf{R}_i \otimes \Delta\mathbf{R}_i = \mathbf{0}, \tag{20}$$

$$\vdots$$

where $\Delta\mathbf{R}_i = \mathbf{R}_i - \mathbf{X}_o$. As can be seen, this is a simultaneous system of linear equations for $\mathbf{x}_o, \mathbf{F}, \mathbf{F}^{(2)}, \ldots, \mathbf{F}^{(m)}$. As expected, when setting the current configuration equal to the initial configuration, we see, by inspection, that the system of equations can be satisfied by taking $\mathbf{x}_o = \mathbf{X}_o$, $\mathbf{F} = \mathbf{I}$, and all the higher gradients as zero. Even though the system might be solved for any order of expansion, in most cases we are interested in first or second gradients. We thus look at the solutions for these expansions.

Let us examine the solution when the expansion includes up to the first deformation gradient, and thus has higher terms truncated. In this case, the system reduces to two equations given by

$$\sum_{i\in\Omega} w_i \left\{\mathbf{r}_i - \mathbf{x}_o - \mathbf{F}\Delta\mathbf{R}_i\right\} = \mathbf{0}, \tag{21}$$

$$\sum_{i\in\Omega} w_i \{\mathbf{r}_i - \mathbf{x}_o - \mathbf{F}\Delta\mathbf{R}_i\} \otimes \Delta\mathbf{R}_i = \mathbf{0}, \tag{22}$$

which can be written as

$$\sum_{i\in\Omega} w_i(\mathbf{r}_i - \mathbf{x}_o) = \mathbf{F}\sum_{i\in\Omega} w_i \Delta\mathbf{R}_i, \tag{23}$$

$$\sum_{i\in\Omega} w_i(\mathbf{r}_i - \mathbf{x}_o) \otimes \Delta\mathbf{R}_i = \mathbf{F}\sum_{i\in\Omega} w_i \Delta\mathbf{R}_i \otimes \Delta\mathbf{R}_i. \tag{24}$$

Expanding around the weighted center of the system in the reference configuration so that

$$\mathbf{X}_o = \frac{1}{w}\sum_{i\in\Omega} w_i \mathbf{R}_i, \tag{25}$$

results in $\sum_{i\in\Omega} w_i \Delta\mathbf{R}_i = \mathbf{0}$ and, thus, the first equation of the system, Eq. (23), states that

$$\mathbf{x}_o = \frac{1}{w}\sum_{i\in\Omega} w_i \mathbf{r}_i. \tag{26}$$

Thus $\mathbf{x}_o$ will be the weighted center of the system in the current configuration. Considering the second equation of the system, Eq. (24), one obtains

$$\mathbf{F} = \left(\sum_{i\in\Omega} w_i(\mathbf{r}_i - \mathbf{x}_o) \otimes \Delta\mathbf{R}_i\right)\left(\sum_{i\in\Omega} w_i \Delta\mathbf{R}_i \otimes \Delta\mathbf{R}_i\right)^{-1}. \tag{27}$$

As can be seen, the existence of the deformation gradient is dependent on the existence of the inverse of the sum

$$\sum_{i\in\Omega} w_i \Delta\mathbf{R}_i \otimes \Delta\mathbf{R}_i. \tag{28}$$

Just by examining this term, one can conclude that MD systems that start with an initial configuration on a flat plane do not allow calculation of a general deformation gradient. This also includes, as a special case, MD systems that start on a straight line or a flat curve. The deformation gradient allows us to define the right and left Cauchy stretch tensors $\mathbf{C} = \mathbf{F}^T\mathbf{F}$ and $\mathbf{B} = \mathbf{F}\mathbf{F}^T$, and the associated Green–Lagrange and Almansi strains. The deformation gradient is fully consistent with the motion of the system so that the deformation gradient rate is

$$\dot{\mathbf{F}} = \left(\sum_{i\in\Omega} w_i(\mathbf{v}_i - \mathbf{v}_o) \otimes \Delta\mathbf{R}_i\right)\left(\sum_{i\in\Omega} w_i \Delta\mathbf{R}_i \otimes \Delta\mathbf{R}_i\right)^{-1}, \tag{29}$$

where $\mathbf{v}_o = \dot{\mathbf{x}}_o$ is the velocity of the weighted center, and in which this deformation gradient rate minimizes the weighted residual between the velocity map and the particle velocities. As a result, a velocity gradient can be defined as

$$\mathbf{L} = \dot{\mathbf{F}}\mathbf{F}^{-1} = \left(\sum_{i\in\Omega} w_i(\mathbf{v}_i - \mathbf{v}_o) \otimes \Delta\mathbf{R}_i\right)\left(\sum_{i\in\Omega} w_i(\mathbf{r}_i - \mathbf{x}_o) \otimes \Delta\mathbf{R}_i\right)^{-1}, \tag{30}$$

which only exists when the inverse exists. That is, as noted before for the reference system, the current system cannot be on a flat plane. A deformation rate $\mathbf{D}$ can be defined as the symmetric part of $\mathbf{L}$ and a vorticity $\mathbf{W}$ defined as its skew-symmetric part.

If we take the weight as unit, then the point of expansion is the centroid of the system in the reference configuration, and $\mathbf{x}_o$ is the centroid of the current system. Then, the deformation gradient is given by

$$\mathbf{F} = \left(\sum_{i\in\Omega} (\mathbf{r}_i - \mathbf{x}_o) \otimes \Delta\mathbf{R}_i\right)\left(\sum_{i\in\Omega} \Delta\mathbf{R}_i \otimes \Delta\mathbf{R}_i\right)^{-1}. \tag{31}$$

On the other hand, if we take the weight as the particle mass, then the point of expansion is the center of mass in the reference configuration, and $\mathbf{x}_o$ is the center of mass in the current configuration. In this case the deformation gradient is

$$\mathbf{F} = \left(\sum_{i\in\Omega} m_i(\mathbf{r}_i - \mathbf{x}_o)\otimes\Delta\mathbf{R}_i\right)\left(\sum_{i\in\Omega} m_i\Delta\mathbf{R}_i\otimes\Delta\mathbf{R}_i\right)^{-1}. \tag{32}$$

As will be shown later, the expression for stress is not necessarily symmetric so we have a natural interest in knowing higher order deformation gradients. For a three-term expansion, the system to solve becomes

$$\sum_{i\in\Omega} w_i\left\{\mathbf{r}_i - \mathbf{x}_o - \mathbf{F}\Delta\mathbf{R}_i - \frac{1}{2}\mathbf{F}^{(2)} : (\Delta\mathbf{R}_i\otimes\Delta\mathbf{R}_i)\right\} = \mathbf{0}, \tag{33}$$

$$\sum_{i\in\Omega} w_i\left\{\mathbf{r}_i - \mathbf{x}_o - \mathbf{F}\Delta\mathbf{R}_i - \frac{1}{2}\mathbf{F}^{(2)} : (\Delta\mathbf{R}_i\otimes\Delta\mathbf{R}_i)\right\}\otimes\Delta\mathbf{R}_i = \mathbf{0}, \tag{34}$$

$$\sum_{i\in\Omega} w_i\left\{\mathbf{r}_i - \mathbf{x}_o - \mathbf{F}\Delta\mathbf{R}_i - \frac{1}{2}\mathbf{F}^{(2)} : (\Delta\mathbf{R}_i\otimes\Delta\mathbf{R}_i)\right\}\otimes\Delta\mathbf{R}_i\otimes\Delta\mathbf{R}_i = \mathbf{0}. \tag{35}$$

This can be reorganized into the system

$$\mathbf{x}_o\sum_{i\in\Omega} w_i + \mathbf{F}\sum_{i\in\Omega} w_i\Delta\mathbf{R}_i + \mathbf{F}^{(2)} : \sum_{i\in\Omega} w_i\Delta\mathbf{R}_i\otimes\Delta\mathbf{R}_i = \sum_{i\in\Omega} w_i\mathbf{r}_i, \tag{36}$$

$$\begin{aligned}&\mathbf{x}_o\otimes\sum_{i\in\Omega} w_i\Delta\mathbf{R}_i + \mathbf{F}\sum_{i\in\Omega} w_i\Delta\mathbf{R}_i\otimes\Delta\mathbf{R}_i + \mathbf{F}^{(2)} : \sum_{i\in\Omega} w_i\Delta\mathbf{R}_i\otimes\Delta\mathbf{R}_i\otimes\Delta\mathbf{R}_i\\ &\quad = \sum_{i\in\Omega} w_i\mathbf{r}_i\otimes\Delta\mathbf{R}_i,\end{aligned} \tag{37}$$

$$\begin{aligned}&\mathbf{x}_o\otimes\sum_{i\in\Omega} w_i\Delta\mathbf{R}_i\otimes\Delta\mathbf{R}_i + \mathbf{F}\sum_{i\in\Omega} w_i\Delta\mathbf{R}_i\otimes\Delta\mathbf{R}_i\otimes\Delta\mathbf{R}_i\\ &\quad + \mathbf{F}^{(2)} : \sum_{i\in\Omega} w_i\Delta\mathbf{R}_i\otimes\Delta\mathbf{R}_i\otimes\Delta\mathbf{R}_i\otimes\Delta\mathbf{R}_i = \sum_{i\in\Omega} w_i\mathbf{r}_i\otimes\Delta\mathbf{R}_i\otimes\Delta\mathbf{R}_i.\end{aligned} \tag{38}$$

By expanding around the weighted center in the reference configuration, then this system reduces to

$$\mathbf{x}_o w + \mathbf{F}^{(2)} : \sum_{i\in\Omega} w_i\Delta\mathbf{R}_i\otimes\Delta\mathbf{R}_i = \sum_{i\in\Omega} w_i\mathbf{r}_i, \tag{39}$$

$$\mathbf{F}\sum_{i\in\Omega} w_i\Delta\mathbf{R}_i\otimes\Delta\mathbf{R}_i + \mathbf{F}^{(2)} : \sum_{i\in\Omega} w_i\Delta\mathbf{R}_i\otimes\Delta\mathbf{R}_i\otimes\Delta\mathbf{R}_i = \sum_{i\in\Omega} w_i\mathbf{r}_i\otimes\Delta\mathbf{R}_i, \tag{40}$$

$$\begin{aligned}&\mathbf{x}_o\otimes\sum_{i\in\Omega} w_i\Delta\mathbf{R}_i\otimes\Delta\mathbf{R}_i + \mathbf{F}\sum_{i\in\Omega} w_i\Delta\mathbf{R}_i\otimes\Delta\mathbf{R}_i\otimes\Delta\mathbf{R}_i\\ &\quad + \mathbf{F}^{(2)} : \sum_{i\in\Omega} w_i\Delta\mathbf{R}_i\otimes\Delta\mathbf{R}_i\otimes\Delta\mathbf{R}_i\otimes\Delta\mathbf{R}_i = \sum_{i\in\Omega} w_i\mathbf{r}_i\otimes\Delta\mathbf{R}_i\otimes\Delta\mathbf{R}_i.\end{aligned} \tag{41}$$

We can now solve for $\mathbf{x}_o$ from the first equation and $\mathbf{F}$ from the second equation in terms of the second-order gradient and substitute them into the third equation. This results in

$$\mathbf{x}_o = \frac{1}{w}\sum_{i\in\Omega} w_i\mathbf{r}_i - \frac{1}{w}\mathbf{F}^{(2)} : \sum_{i\in\Omega} w_i\Delta\mathbf{R}_i\otimes\Delta\mathbf{R}_i, \tag{42}$$

$$\mathbf{F} = \left(\sum_{i\in\Omega} w_i\mathbf{r}_i\otimes\Delta\mathbf{R}_i - \mathbf{F}^{(2)} : \sum_{i\in\Omega} w_i\Delta\mathbf{R}_i\otimes\Delta\mathbf{R}_i\otimes\Delta\mathbf{R}_i\right)\left(\sum_{i\in\Omega} w_i\Delta\mathbf{R}_i\otimes\Delta\mathbf{R}_i\right)^{-1}. \tag{43}$$

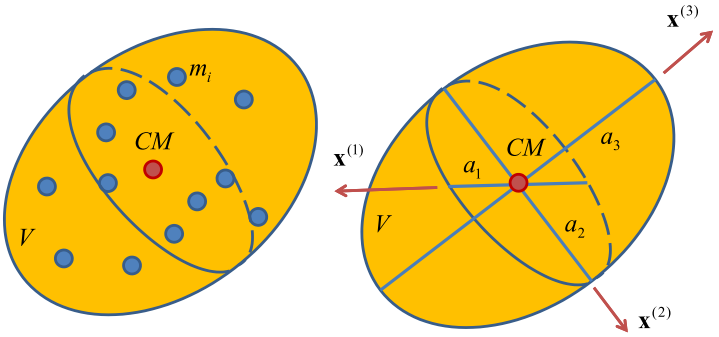

Fig. 4. Equivalent uniform ellipsoid to the MD system.

What is immediately obvious is that $\mathbf{x}_o$ is no longer the weighted center in the current configuration. Also, the process has altered the deformation gradient too, a characteristic of fitting with non-orthogonal functions. Yet, we still need the inverse to exist, which excludes systems that initially fall on a flat plane.

Because the systems are linear in the unknowns, they can be systematically solved for higher gradients, contingent on the existence of a solution.

3.2. Stress measure

This section defines a Cauchy stress tensor $\mathbf{T}$, similar to that used in continuum mechanics, from which a traction vector $\mathbf{t}^{(n)}$ on a surface with unit normal $\mathbf{n}$ is defined by the Cauchy relation

$$\mathbf{t}^{(n)} = \mathbf{n}\mathbf{T}. \tag{44}$$

Ideally, this Cauchy stress-like measure should be related and derived from a selected set of particles in a MD simulation. This can be done by calculating a stress tensor that minimizes the difference between all traction forces calculated from the stress tensor and the corresponding tractions calculated from the particle interactions in the MD system. The resulting stress is a second-order tensor, but not necessarily symmetric.

To calculate the traction force $\mathbf{P}^{(n)}$ on the surface with normal $\mathbf{n}$ from the stress tensor, the associated traction vector $\mathbf{t}^{(n)}$ should be multiplied by a representative area A associated with the molecular system in the MD simulation. Therefore, an area associated with normal must be defined for the molecular system. This is done by considering a uniform mass in the shape of an ellipsoid selected to be equivalent to the MD system, see Fig. 4. The idea here is to construct an ellipsoid of constant density that is centered at the center of mass of the selected particles, and that has equal mass and equal mass moment of inertia. In the case of the MD system the total mass is obtained from adding the mass of the particles, and the mass moment of inertia is calculated from

$$\bar{\mathbf{I}}_m = \sum_{i\in\Omega} m_i \left[(\boldsymbol{\rho}_i \circ \boldsymbol{\rho}_i)\mathbf{I} - \boldsymbol{\rho}_i \otimes \boldsymbol{\rho}_i\right], \tag{45}$$

where $\boldsymbol{\rho}_i$ is the relative position of particle i to the center of mass, and $\mathbf{I}$ is the second-order identity tensor, see Fig. 1. The three eigenvalues of $\bar{\mathbf{I}}_m$ are denoted by $\bar{I}_i$ and the corresponding normalized eigenvectors by $\mathbf{x}^{(i)}$. The eigenvectors provide the transformation that takes us to the spectral representation of $\bar{\mathbf{I}}_m$, in which the tensor is represented as

$$\bar{\mathbf{I}}_m = \bar{I}_1\mathbf{x}^{(1)} \otimes \mathbf{x}^{(1)} + \bar{I}_2\mathbf{x}^{(2)} \otimes \mathbf{x}^{(2)} + \bar{I}_3\mathbf{x}^{(3)} \otimes \mathbf{x}^{(3)}. \tag{46}$$

As shown in Fig. 4, an equivalent ellipsoid is considered that is uniform and has the same mass and mass moment of inertia as the MD system. The volume of the equivalent ellipsoid with principal axes of length a_i and principal directions $\mathbf{x}^{(i)}$ is given by

$$V = \frac{4\pi}{3} a_1 a_2 a_3, \tag{47}$$

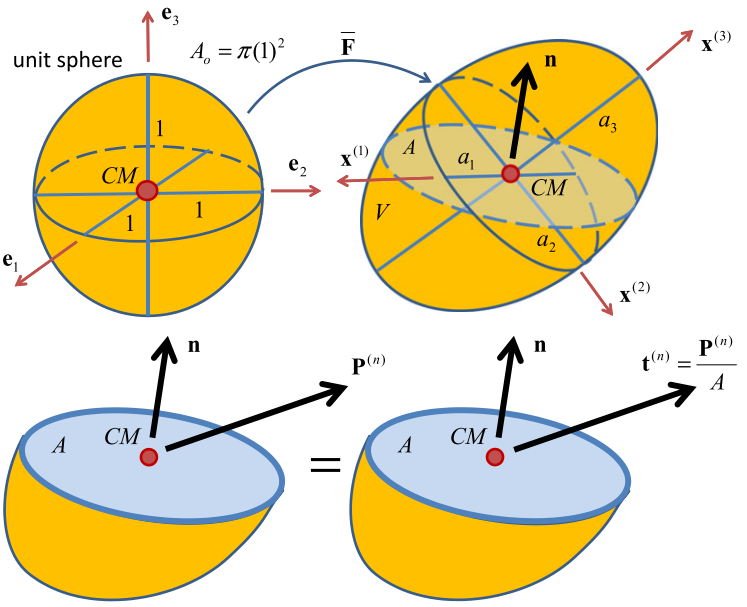

Fig. 5. Equivalent traction vector and corresponding traction load calculated using cuts in the equivalent ellipsoid.

and its mass moment of inertia in the principal coordinates is given by

$$[\bar{\mathbf{I}}_m] = \frac{m}{5}\begin{bmatrix} a_2^2 + a_3^2 & 0 & 0 \\ 0 & a_1^2 + a_3^2 & 0 \\ 0 & 0 & a_1^2 + a_2^2 \end{bmatrix}_{\mathbf{x}^{(i)}}. \tag{48}$$

To make this uniform ellipsoid equivalent to the MD system, the ellipsoid density ρ and volume V must relate through the equation $m = \rho V$. In addition, the principal moments of inertia should be the same for the two. By matching these one obtains

$$\begin{Bmatrix} \bar{I}_1 \\ \bar{I}_2 \\ \bar{I}_3 \end{Bmatrix} = \frac{m}{5}\begin{bmatrix} 0 & 1 & 1 \\ 1 & 0 & 1 \\ 1 & 1 & 0 \end{bmatrix}\begin{Bmatrix} a_1^2 \\ a_2^2 \\ a_3^2 \end{Bmatrix}. \tag{49}$$

Solving this system one obtains

$$\begin{Bmatrix} a_1^2 \\ a_2^2 \\ a_3^2 \end{Bmatrix} = \frac{5}{2m}\begin{Bmatrix} -\bar{I}_1 + \bar{I}_2 + \bar{I}_3 \\ \bar{I}_1 - \bar{I}_2 + \bar{I}_3 \\ \bar{I}_1 + \bar{I}_2 - \bar{I}_3 \end{Bmatrix}. \tag{50}$$

As shown in Fig. 5, the ellipsoid can be mapped from a unit sphere. We will denote this transformation as $\bar{\mathbf{F}}$. It is given by the expression

$$\bar{\mathbf{F}} = a_1\mathbf{x}^{(1)} \otimes \mathbf{e}_1 + a_2\mathbf{x}^{(2)} \otimes \mathbf{e}_2 + a_3\mathbf{x}^{(3)} \otimes \mathbf{e}_3, \tag{51}$$

where $\mathbf{e}_i$ is an orthonormal base for the sphere that transforms into the ellipsoid with principal directions along the normalized eigenvectors $\mathbf{x}^{(i)}$ of the mass moment of inertia $\bar{\mathbf{I}}_m$. The relation between the surface exposed by cutting the ellipsoid with a surface of normal $\mathbf{n}$ passing through the centroid, as shown in Fig. 5, and its corresponding surface in the unit sphere is known from continuum mechanics (see Ref. [41]), and given by

$$\frac{dA}{dA_o} = \sqrt{\frac{\det(\bar{\mathbf{B}})}{\mathbf{n} \circ (\bar{\mathbf{B}}\mathbf{n})}}, \tag{52}$$

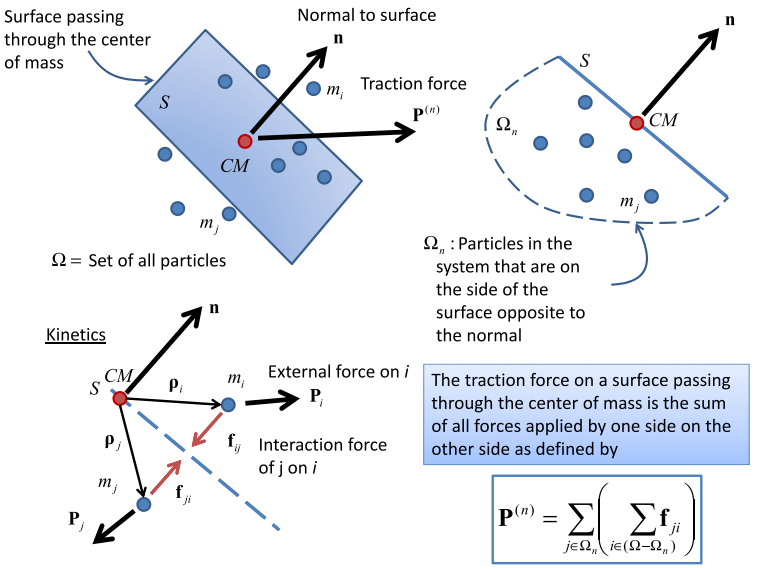

Fig. 6. The traction force on part of the system.

where $\bar{\mathbf{B}} = \bar{\mathbf{F}}\bar{\mathbf{F}}^T$ is given by

$$\bar{\mathbf{B}} = a_1^2\mathbf{x}^{(1)} \otimes \mathbf{x}^{(1)} + a_2^2\mathbf{x}^{(2)} \otimes \mathbf{x}^{(2)} + a_3^2\mathbf{x}^{(3)} \otimes \mathbf{x}^{(3)}. \tag{53}$$

Since the transformation is homogeneous, flat surfaces transform as flat surfaces. Therefore, the surface corresponding to the cut of the ellipsoid is a flat surface in the unit sphere. This surface has an area π. As a result of the homogeneous characteristics of $\bar{\mathbf{F}}$, the area of surface obtained by cutting the ellipsoid is given by

$$A = \pi\sqrt{\frac{\det(\bar{\mathbf{B}})}{\mathbf{n} \circ (\bar{\mathbf{B}}\mathbf{n})}}. \tag{54}$$

One can easily show that $\det(\bar{\mathbf{B}}) = a_1^2a_2^2a_3^2$ and that $\mathbf{n} \circ (\bar{\mathbf{B}}\mathbf{n}) = a_i^2(\mathbf{x}^{(i)} \circ \mathbf{n})^2 = a_i^2\cos^2\theta_i$, where $\cos\theta_i$ are the direction cosines of $\mathbf{n}$ in the base of the principal directions of $\bar{\mathbf{I}}_m$. This leads to

$$A = \pi\sqrt{\frac{a_1^2a_2^2a_3^2}{a_1^2\cos^2\theta_1 + a_2^2\cos^2\theta_2 + a_3^2\cos^2\theta_3}}. \tag{55}$$

As shown in Fig. 5, the traction vector $\mathbf{t}^{(n)}$ is the load per unit area. It can be calculated either from the Cauchy relation $\mathbf{t}^{(n)} = \mathbf{n}\mathbf{T}$ or from the MD system by dividing the calculated traction load $\mathbf{P}^{(n)}$ by a representative area A so that

$$\mathbf{t}^{(n)} = \frac{1}{A}\mathbf{P}^{(n)}. \tag{56}$$

In this calculation the representative area is the area of the cut through the center of mass of the equivalent ellipsoid by a surface with normal $\mathbf{n}$. As shown in Fig. 6, to get the MD load $\mathbf{P}^{(n)}$, we cut the system by a surface with normal $\mathbf{n}$ and passing through the center of mass of the MD system. The load $\mathbf{P}^{(n)}$ is defined as the total load applied by the particles of one side, the side that $\mathbf{n}$ is pointing toward, on the particles of the other side, and given by

$$\mathbf{P}^{(n)} = \sum_{j\in\Omega_n}\left(\sum_{i\in(\Omega-\Omega_n)}\mathbf{f}_{ji}\right). \tag{57}$$

Newton's third law simplifies this to

$$\mathbf{P}^{(n)} = \sum_{j\in\Omega_n}\left(\sum_{i\in\Omega}\mathbf{f}_{ji}\right). \tag{58}$$

To calculate the optimum Cauchy stress $\mathbf{T}$ for the MD system, the difference between the traction calculated by the Cauchy relation and that calculated from the MD system is minimized over all possible cuts of the MD system by surfaces passing through its center of mass. This difference for a single cut is denoted by $\mathbf{\Delta}^{(n)}$ and defined by the relation

$$\mathbf{\Delta}^{(n)} = \frac{1}{A}\mathbf{P}^{(n)} - \mathbf{nT}. \tag{59}$$

The total residual over all cuts, defined in a least-square sense, is given by

$$R = \frac{1}{2}\int_S \mathbf{\Delta}^{(n)} \circ \mathbf{\Delta}^{(n)} dS, \tag{60}$$

where the residual is weighted for each normal $\mathbf{n}$ by a corresponding differential area dS on the surface S of a sphere. This is one way to force equal weighting for residuals along different directions. Since the goal is to find the stress $\mathbf{T}$ that minimizes the total residual, the gradient $\partial_{\mathbf{T}}(R)$ is calculated and set to zero to obtain the equation

$$\int_S \mathbf{\Delta}^{(n)} \circ \partial_{\mathbf{T}}(\mathbf{\Delta}^{(n)}) dS = \mathbf{0}. \tag{61}$$

As $\mathbf{\Delta}^{(n)}$ is linear in the stress $\mathbf{T}$, it follows that

$$\partial_{\mathbf{T}}(\mathbf{\Delta}^{(n)}) = -\mathbf{nII}, \tag{62}$$

where $\mathbf{II}$ is the fourth-order identity ($\mathbf{II} : \mathbf{A} = \mathbf{A}$ for every second-order tensor $\mathbf{A}$). Substituting this into (61), using the identity $\mathbf{a} \circ (\mathbf{bII}) = \mathbf{b} \otimes \mathbf{a}$, for any two vectors $\mathbf{a}$ and $\mathbf{b}$, and noting that the stress $\mathbf{T}$ is constant give

$$\int_S (\mathbf{n} \otimes \mathbf{n})\, dS\mathbf{T} = \int_S \frac{1}{A}\mathbf{n} \otimes \mathbf{P}^{(n)} dS. \tag{63}$$

Using the divergence theorem on a sphere of radius r gives

$$\int_S (\mathbf{n} \otimes \mathbf{n})\, dS = \frac{V_s}{r}\mathbf{I}, \tag{64}$$

where V_s is the volume of the sphere defined by S. Introducing this yields the expression for the optimal Cauchy stress for the MD system as

$$\mathbf{T} = \frac{r}{V_s}\int_S \frac{1}{A}\mathbf{n} \otimes \mathbf{P}^{(n)} dS. \tag{65}$$

Since the role of the integration surface S is to help equally weight the residual from different surfaces, we can take S to represent a unit sphere for which $V_s = 4\pi/3$. Introducing this, using Eq. (54), and noting $\det(\bar{\mathbf{B}})$ is constant finally yield

$$\mathbf{T} = \frac{3}{4\pi^2\sqrt{\det(\bar{\mathbf{B}})}}\int_S \sqrt{\mathbf{n} \circ (\bar{\mathbf{B}}\mathbf{n})}\mathbf{n} \otimes \mathbf{P}^{(n)} dS. \tag{66}$$

The selection of the equivalent uniform ellipsoid clearly provides a method to identify areas needed for the definition of the traction, and from that the determination of stress. This is an approximation that influences the scale of the stress. This can be seen when comparing the dimensions associated with other shapes to that associated with the ellipsoid. For this consider Table 1 which shows several objects including a rectangular prism, a solid cylinder, a hollow cylinder, a cylindrical shell, and a spherical shell. The principal directions of the equivalent ellipsoid are selected to be $\mathbf{e}_i$ and aligned with the directions of the shape, and with A_{e_i} denoting the area of the ellipsoid exposed

Table 1
Equivalent ellipsoids for basic shapes relative to the common center of mass and principal direction aligned with that of the given shape.

Shape	Dimensions	Equivalent ellipsoid	Principal area ratios
Solid rectangular prism	b_1, b_2, b_3	$a_i = \sqrt{\frac{5}{12}} b_i$	$\frac{5\pi}{12} \approx 1.31$
Solid cylinder along 1-axis	r, L	$a_1 = \sqrt{\frac{5}{12}} L$	$\frac{Ae_1}{\pi r^2} = 1.25$
		$a_2 = a_3 = \sqrt{\frac{5}{4}} r$	$\frac{Ae_2}{2rL} = \frac{5\pi}{8\sqrt{3}} \approx 1.13$
Hollow cylinder along 1-axis	r_i, r_o, L	$a_1 = \sqrt{\frac{5}{12}} L$	$\frac{Ae_1}{\pi(r_o^2 - r_i^2)} = 1.25 \frac{r_o^2 + r_i^2}{r_o^2 - r_i^2}$
		$a_2 = a_3 = \sqrt{\frac{5}{4}(r_o^2 + r_i^2)}$	$\frac{Ae_2}{2(r_o - r_i)L} = \frac{5\pi\sqrt{r_o^2 + r_i^2}}{8\sqrt{3}(r_o - r_i)}$
Spherical shell	r	$a_i = \sqrt{\frac{5}{3}} r$	$\frac{Ae_i}{\pi r^2} = \frac{5}{3} \approx 1.67$
Cylindrical shell along 1-axis without end caps	r, L	$a_1 = \sqrt{\frac{5}{12}} L$	$\frac{Ae_1}{\pi r^2} = 2.5$
		$a_2 = a_3 = \sqrt{\frac{5}{2}} r$	$\frac{Ae_2}{2rL} = \frac{5\pi}{4\sqrt{6}} \approx 1.60$

by passing a plane with normal $\mathbf{e}_i$ through its centroid. Obviously, a solid sphere and the solid ellipsoid are modeled exactly, but as can be seen from the table, the areas obtained by cutting the equivalent ellipsoid can be significantly different when the particles pack into spaces that resemble, for example, a cylindrical shell.

3.3. Nominal and Cauchy stress

A Cauchy stress has been defined based on the idea of an equivalent ellipsoid, set at the center of mass of the MD system, and with identical mass and mass moment of inertia. With some additional assumptions, one could follow the same ideas and similar procedures to produce a nominal stress that would use the system in the current configuration and the corresponding areas in the reference configuration. Let the mass moment of inertia of the MD system in the reference configuration be $\bar{\mathbf{I}}_{mo}$. From this one can find a corresponding ellipsoid of uniform density and then can calculate the cross-sectional areas A_o corresponding to cuts with unit normal $\mathbf{N}$. Since the traction load $\mathbf{P}^{(n)}$ is given only in the current configuration for a surface with normal $\mathbf{n}$, we need to identify a surface in the reference configuration that corresponds with this surface in the current configuration. This is done by assuming that the normals corresponding to similar surfaces in the reference and current configurations are related by the deformation gradient through the standard relation from continuum mechanics of continuous systems, see Ref. [41], written as

$$\mathbf{N} = \frac{1}{\det(\mathbf{F})} \sqrt{\frac{\det^2(\mathbf{F})}{\mathbf{n} \circ (\mathbf{B}\mathbf{n})}} \mathbf{n}\mathbf{F}, \tag{67}$$

$$\mathbf{n} = \frac{\det(\mathbf{F})}{\sqrt{\det^2(\mathbf{F}) \mathbf{N} \circ (\mathbf{C}^{-1}\mathbf{N})}} \mathbf{F}^{-T}\mathbf{N}. \tag{68}$$

One can now define the nominal traction for the MD system as the current traction load $\mathbf{P}^{(n)}$ divided by the area A_o corresponding to a cut of the reference ellipsoid by a surface with normal $\mathbf{N}$ defined by (67). By minimizing the difference between this traction and the traction calculated by the nominal stress $\mathbf{T}_o$, following similar procedures as before, for a sphere of radius r and volume V_s, one obtains

$$\mathbf{T}_o = \frac{r}{V_s} \int_S \frac{1}{A_o} \mathbf{N} \otimes \mathbf{P}^{(n)} dS. \tag{69}$$

Since the MD system does not actually deform as a continuum, the resulting nominal stress calculated here is different from that which would be obtained from the Cauchy stress (66) using the well-known continuum mechanics relation

$$\mathbf{T}_o = \det(\mathbf{F}) \mathbf{F}^{-1} \mathbf{T}. \tag{70}$$

In particular, A_o is not related to A through the continuum mechanics relation

$$\frac{A}{A_o} = \det(\mathbf{F})\sqrt{\mathbf{N} \circ (\mathbf{C}^{-1}\mathbf{N})}, \tag{71}$$

since it is independently calculated from cutting an ellipsoid similar to $\bar{\mathbf{I}}_{mo}$, which is calculated from the reference MD system. In this case, the integration over a unit sphere yields

$$A_o = \pi\sqrt{\frac{\det(\bar{\mathbf{B}}_o)}{\mathbf{N} \circ (\bar{\mathbf{B}}_o\mathbf{N})}}, \tag{72}$$

to give, for a sphere of unit radius, the nominal stress as

$$\mathbf{T}_o = \frac{3}{4\pi^2\sqrt{\det(\bar{\mathbf{B}}_o)}}\int_S \sqrt{\mathbf{N} \circ (\bar{\mathbf{B}}_o\mathbf{N})}\mathbf{N} \otimes \mathbf{P}^{(n)} dS. \tag{73}$$

The nominal stress can thus be directly calculated using (73), or we can calculate a nominal stress from the continuum mechanics relation (70). These two definitions will normally result in different values for the nominal stress since the first is based on a minimization that uses the positions in the reference configuration, while the latter is based on using the positions in the current configuration. One could also use the MD definition for the nominal stress given in (73) and use the continuum mechanics relation (70) to get a corresponding Cauchy stress, but again this would not be identical to the one directly obtained in (66) from the MD system.

4. Demonstration of method

There is a difference between the proposed stress, which is given by Eq. (66) and that is obtained by minimizing the difference between the MD and continuum traction when using the equivalent ellipsoid (MinT-EE method), and, for example, the virial stress (6). In addition to the difference in their motivation, the virial stress normalizes the terms using a characteristic volume of the system that needs to be selected by the user. This allows the user to change the shape of the characteristic volume based on the specific problem. This choice is not required for the proposed MinT-EE stress, and, as a result, the values of this stress might be different from those expected for a specific geometric distribution of atoms. This is seen in Fig. 7 for the extension of a nano-tube, which, for the most part, has its atoms on a cylindrical sheet. A comparison of the evaluated MinT-EE axial stresses and the virial stress shows that the virial stress is over twice as large as the MinT-EE stress proposed here. This result is directly related to the selection of the equivalent ellipsoid, which has a cross-sectional area that is over twice that of the nano-tube (see the area ratio for the cylindrical shell in Table 1). A comparison of the moduli in this case shows a modulus of 422 GPa for the MinT-EE as opposed to 644 GPa for the virial stress calculation. The strains in this and the following figures are calculated from the deformation gradient proposed here by the minimization of the difference between the motion of the continuum and that of the particles in the MD system (MinD process) truncating the approximation of the motion after the first deformation gradient. The strains plotted are obtained from the MinD deformation gradient $\mathbf{F}$ by calculating the Green–Lagrange strain $\mathbf{E} = \frac{1}{2}(\mathbf{C} - \mathbf{I})$ and extracting the axial term.

Fig. 8 shows the stress–strain response for multi-layered graphene sheets. As can be seen, the virial stress is approximately the same as the MinT-EE stress. In this case they should be close since the MD system approximately fills a box and the area ratio for the ellipsoid with respect to the box is approximately 1.3, as seen in Table 1 for the rectangular prism.

Fig. 9 shows the axial stress resulting from pulling a multi-layered nano-tube. Included are the proposed MinT-EE stresses for the individual tubes and the system as a whole.

There are many more complex systems that can take advantage of the proposed method. As another example, we consider an ion channel in the cell membrane. The physiological function of these ion channels is to selectively allow a given type of ion to pass through the cell membrane. Fig. 10 shows a potassium channel KcsA (PDB: 1K4C [42]) embedded in a fully hydrated membrane. KcsA belongs to a family of channels found in almost all organisms. These channels have diverse functions and have been implicated in osmotic regulation and neuronal signaling. The system is composed of channel protein, membrane, water and ions. The system is highly inhomogeneous, thus ideally suited for analysis using the proposed MinD procedures for obtaining component deformation.

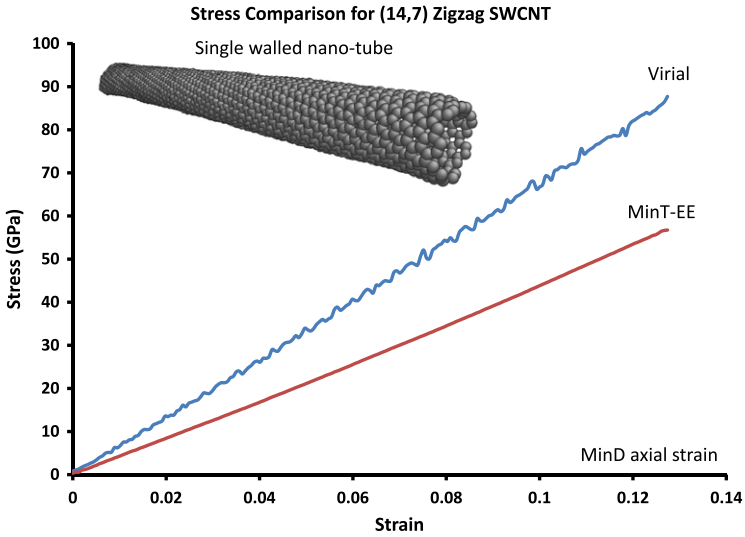

Fig. 7. Axial stress–strain response of a single walled nano-tube during uniaxial extension along the tube axis comparing the virial stress and the proposed MinT-EE stress.

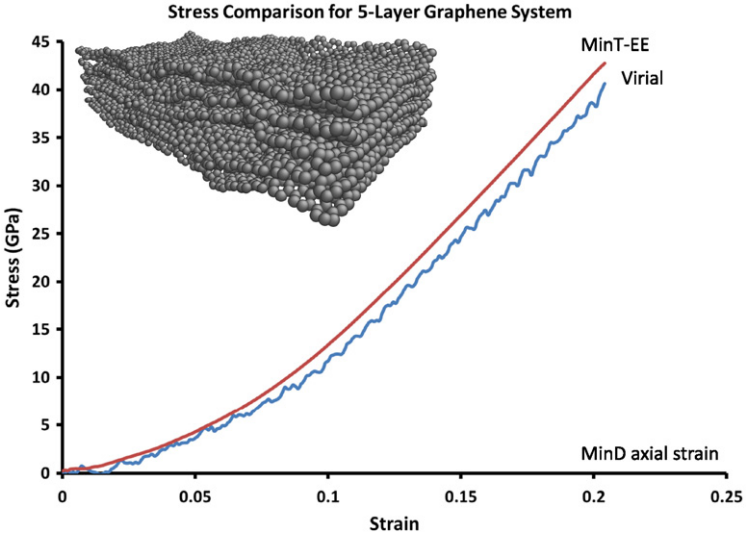

Fig. 8. The stress–strain response during uniaxial extension of a system of graphene sheets comparing the virial stress and the proposed MinT-EE stress.

The opening of potassium channels allows cations to flow passively across the membrane. Although ion flow is fast, ion channels are highly selective, see review by Choe [43]. Ion selectivity takes place at the narrowest part of the ion-permeation pathway, known as the selectivity filter. Doyle et al. [44] reported the first crystal structure of an ion selective filter, using the bacterial potassium channel KcsA as a model system. Their study built the foundation for understanding mechanisms of ion selectivity process and permeation.

Fig. 11 shows the blast impact of the KcsA channel protein–membrane complex showing how the response of the bulk system (and more specifically its strain components) is different from the channel protein, allowing one to study the collapse of this regulating gate of the cell. This can provide information on ultrastructural and molecular changes and the altered activity of ion channels in the demyelinated axon following trauma, as reviewed by Nashmi et al. [45]. See Williamson et al. [46] for detail information on KcsA structural features, channel gating mechanism and its interaction with the surrounding lipid bilayer.

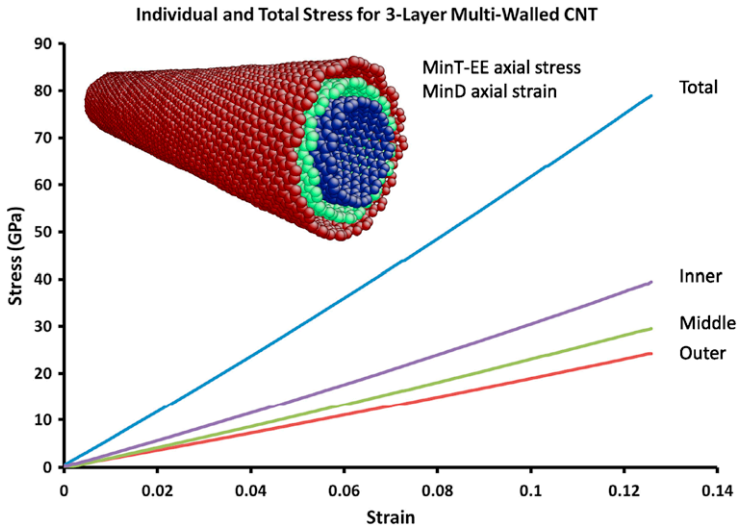

Fig. 9. The axial stress–strain response of a multi-layered nano-tube using the proposed MinT-EE for the individual tubes and for the combined system.

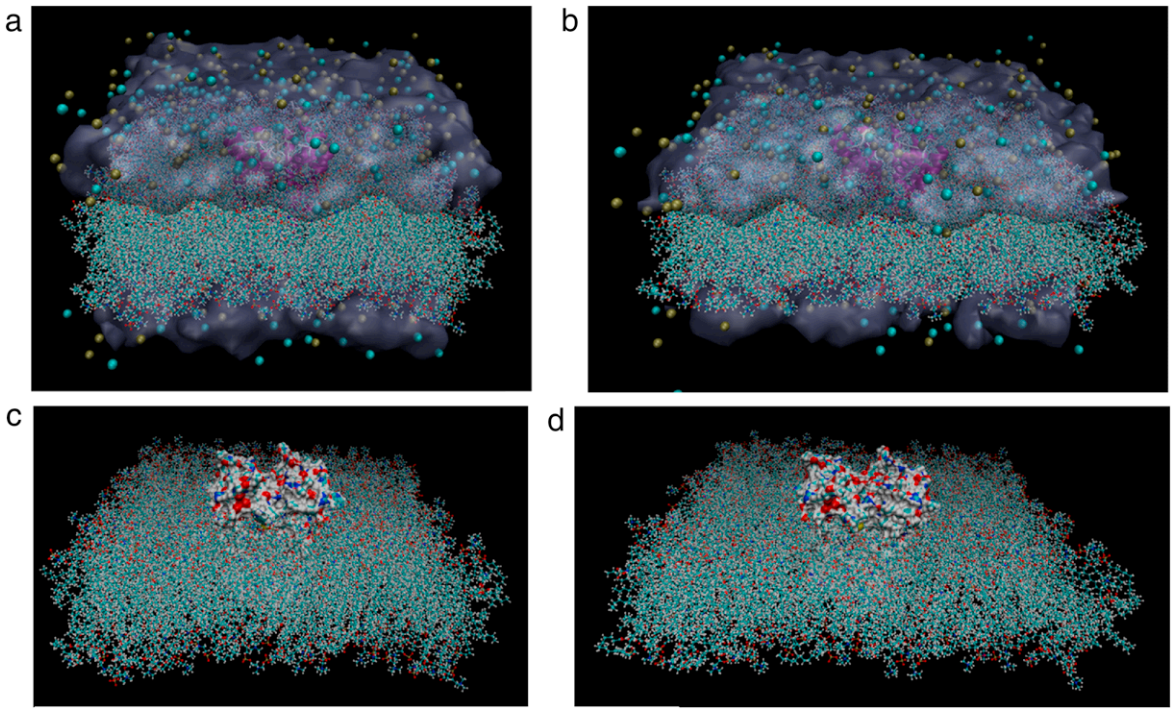

Fig. 10. A potassium channel KcsA (PDB: 1K4C) embedded in a fully hydrated membrane: (a) Complete Channel–Membrane Complex before compression; (b) Complete Channel–Membrane Complex after compression; (c) Channel–Membrane alone before compression; (d) Channel–Membrane after compression.

Another example using the MinD procedure to evaluate the response of a MD system is shown in Fig. 12. In this case we are considering the uniaxial extension of a polycarbonate (PC) system consisting of 80 molecules, each one consisting of 30 monomers (repeating units). The simulation is an all-atom simulation, using the polymer consistent force field (PCFF) that was also used for the nano-tubes and the graphene sheet. PCFF is a member of the consistent family of force fields and is used for polymer and organic materials in calculations of cohesive energies, mechanical

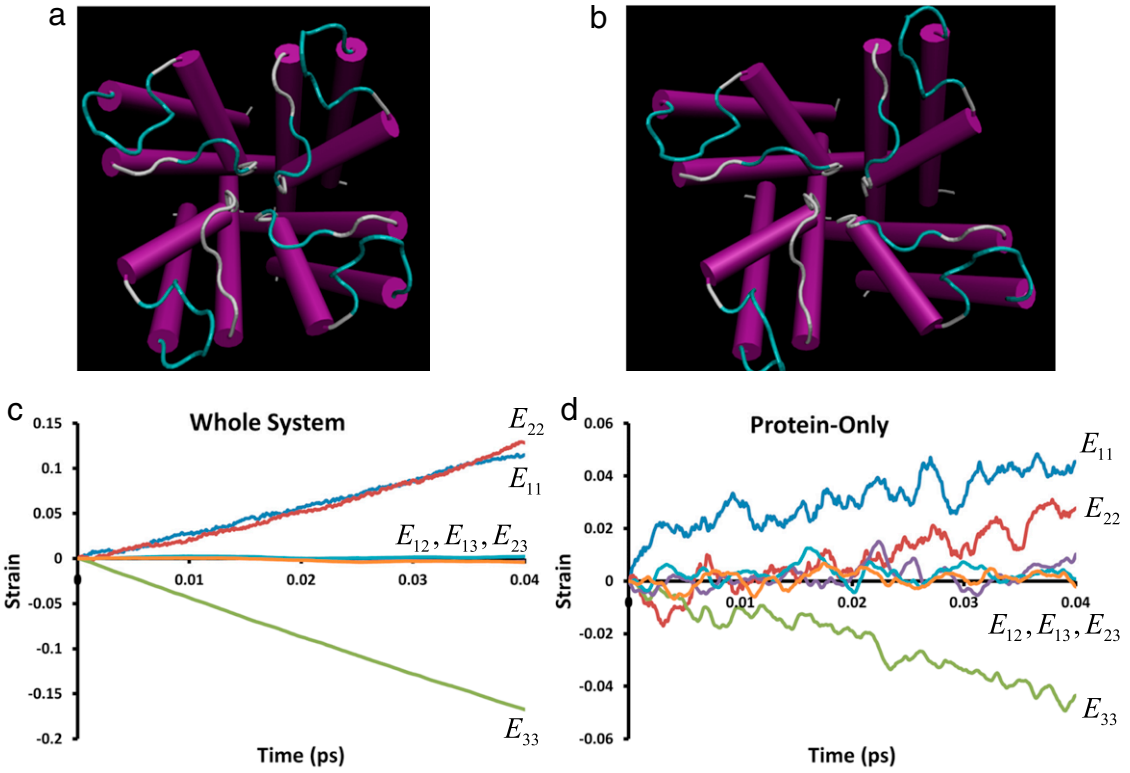

Fig. 11. Rapid compression of a KcsA ion channel system: (a) protein channel before compression; (b) protein channel after compression; (c) MinD Green–Lagrange strain histories for the whole system; (d) MinD Green–Lagrange strain of protein channel.

properties, compressibility, heat capacities, and elastic constants. The PCFF force fields include 12 bonded and 2 non-bonded interactions. The simulation was conducted at 300 K, at a rate of 10^9 s^{-1}, after an initial equilibration process. Even though the macromolecular chains are entangled and sometimes wrapped in and out of the periodic simulation box (see Fig. 12(b)), a deformation gradient can be defined for each chain as well as for the bulk (entire system). As can be seen in Fig. 12(c), the volumetric strain calculated using the MinD process shows that the bulk undergoes an elastic expansion followed by a quasi-constant volumetric strain, characteristic of plastic flow. In contrast, even though the molecules, on average, initially show an expansion, once the volume of the system is large enough to allow non-affine motion, they start to contract volumetrically. However, the axial strains calculated by the MinD process show that the bulk undergoes a constant rate of extension similar to that imposed on the simulation box, and that the average axial strain of the molecules tracks this extension with a slightly lower rate. In these simulations the volumetric strain was calculated from $\epsilon_V = \det(\mathbf{F}) - 1$ and the axial strain was taken as the axial component of the displacement gradient. This definition of the axial strain was used to directly match the simple definition of strain as the change in length per unit initial length, which was used for calculating the strain of the simulation box.

The calculation of the stress using the MinT-EE method is substantially more involved than the double summation required for calculating the virial stress given in (6). In particular, the MinT-EE method would require the calculation of the mass and mass moment of inertia, eigenvalues and eigenvectors of the mass moment of inertia, and the quadrature described in (66). The computational cost of the first three steps in the MinT-EE method is minimal as the number of calculations grows linearly with the number of particles, compared to the cost associated with the quadrature that grows quadratically with the number of quadrature points. For large systems, a comparative estimate of the computational cost to calculate the two stresses can be obtained by looking at the highest order terms in the number of calculations. When considering the number of operations for a n-particle system, the highest order terms for the virial stress include $4.5n^2$ multiplications and $2n^2$ additions, while the MinT-EE method involves $0.25n^2$ additions for each integration point on the sphere. This suggests that for large systems with fewer than 26 integration points in the MinT-EE method, the MinT-EE method is less costly than the virial stress method.

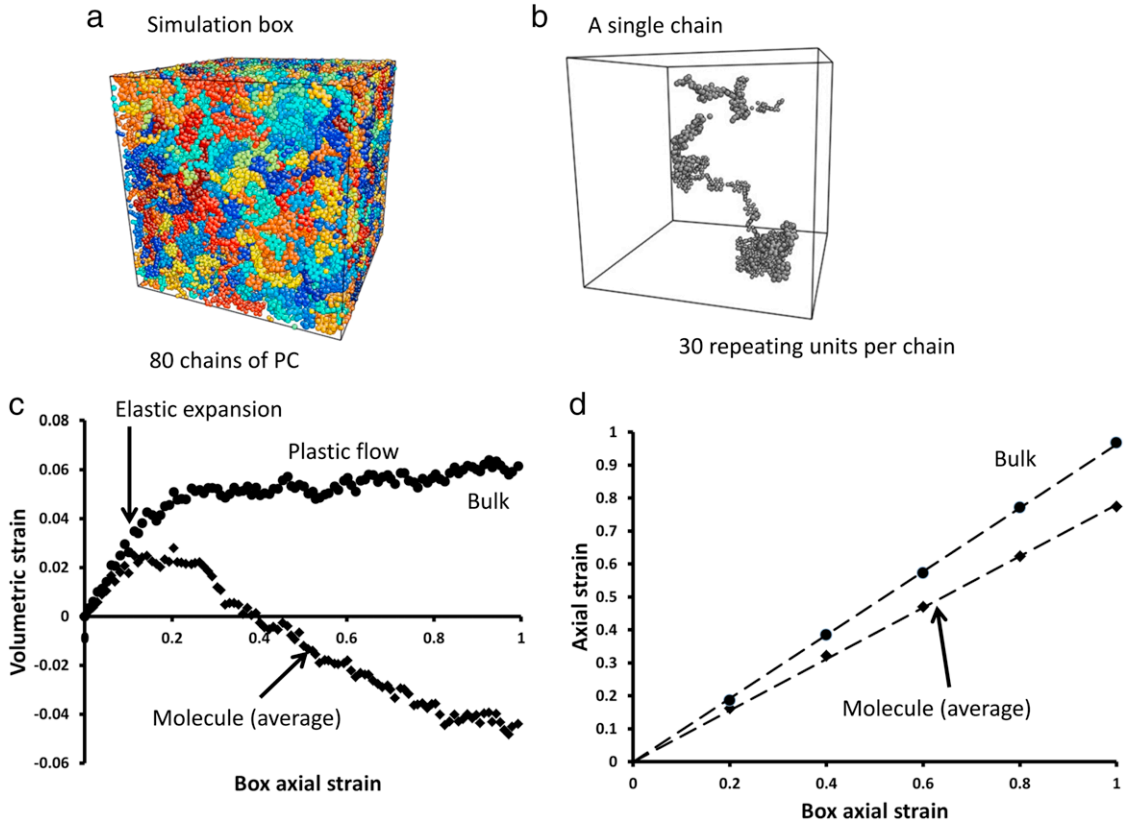

Fig. 12. All-atom simulation of uni-axial extension of a PC system: (a) the simulation box contains 80 PC chains; (b) a single chain constructed of 30 repeating units of the PC monomer; (c) the MinD procedure volumetric strain for the bulk and the average for the molecules; (d) the MinD procedure axial strain for bulk and the averaged value for the molecules ((c) and (d) plotted against the simulation box axial strain).

5. Summary and conclusion

In an effort to connect MD simulations to continuum models, we have developed methods to extract deformation and stress measures that are based on minimizing the difference between identical quantities at the continuum and MD levels.

The kinematic ideas of deformation and its gradients presented here are built on a method recently proposed in the articles [23,24] in which the difference of the continuum mapping and the actual molecular motion is minimized in a least-square sense. In this case we use the weighted average location of the molecular system to expand the continuum deformation mapping around, while in Refs. [23,24] they used an atom location. The result is a slightly different set of equations, that are solved to get the corresponding continuum kinematics. As expected, different results are obtained when including higher gradients in the modeling of the continuum motion. In particular, when truncating the expansion after the first gradient of deformation we note that the average location in the initial system directly maps to the average location in the current configuration, while this is not true when higher terms are included.

In a manner similar to that used for the deformation, the procedure for calculating stress is set up to minimize the difference between the tractions computed from the molecular system and that resulting from a continuum stress (MinT method). To this end, an equivalent continuum volume for the MD system was defined. An equivalent uniform ellipsoid to the MD system was selected that has the same mass and mass moment of inertia. This was then used to calculate the areas associated with each surface passing through the center, set at the center of mass of the MD system. The minimization of the difference was done in a least-square sense over a unit sphere to give identical weights to all directions in space.

The use of an equivalent solid ellipsoid provides an objective way to define both the load and the area that are inherently a part of the notion of the continuum traction, and thus the continuum-level stress. The selection of the

equivalent ellipsoid is not unique so the proposed MinT method can be developed with other uniform solid shapes that have equivalent mass and mass moment of inertia to the MD system.

The influence of selecting the equivalent solid ellipsoid was briefly demonstrated by studying the stress–strain responses of several nano-structures. Graphene sheets, that produce an equivalent ellipsoid that is close to the size of the system, and single and multi-layered nano-tubes, which produce equivalent ellipsoids that can be substantially larger than the dimensions of the tubes, were first considered. The resulting stress for the single walled nano-tube is thus smaller than expected, but this difference decreases with the increase in the number of layers in the nano-tube as the atomic structure approaches a uniformly packed system. A much more complex heterogeneous system associated with ion transfer through the outer membrane of a biological cell during high rate loading was briefly illustrated.

Acknowledgments

The research has been partially supported by the US Army Research Laboratory through Contract Number W911NF-11-D-0001-0094. Lili Zhang and Antoine Jérusalem acknowledge funding from the European Research Council under the European Union's Seventh Framework Program (FP7 2007–2013)/ERC Grant Agreement No. 306587. John Jasa would like to acknowledge the support of the Undergraduate Creative Activities and Research Experience (UCARE) program at the University of Nebraska-Lincoln.

Mehrdad Negahban would like to acknowledge and thank Dr. Stewart A. Silling for helping authors find the articles of Gullett et al. [23] and Zimmerman et al. [24] that have based their development for the deformation on similar procedures as presented here.

References

[1] R. Clausius, Ueber einen auf die Wärme anwendbaren mechanischen Satz, Ann. Phys. 217 (9) (1870) 124–130.
[2] J.H. Irving, J.G. Kirkwood, The statistical mechanical theory of transport processes. IV. The equations of hydrodynamics, J. Chem. Phys. (1950) 817.
[3] R.J. Hardy, Formulas for determining local properties in molecular dynamics simulations: shock waves, J. Chem. Phys. 76 (1982) 622.
[4] M.E. Tuckerman, Statistical Mechanics: Theory and Molecular Simulation, Oxford University Press, USA, 2010.
[5] E.B. Tadmor, R.E. Miller, Modeling Materials: Continuum, Atomistic and Multiscale Techniques, Cambridge University Press, 2012.
[6] S. Plimpton, Fast parallel algorithms for short-range molecular dynamics, J. Comput. Phys. 117 (1995) 1–19.
[7] Sandia National Laboratory, Large-scale Atomic/Molecular Massively Parallel Simulator (LAMMPS), http://lammps.sandia.gov.
[8] Theoretical Biophysics Group, University of Illinois and Beckman Institute, NAMD Scalable Molecular Dynamics, http://www.ks.uiuc.edu/Research/namd/.
[9] W. Humphrey, A. Dalke, K. Schulten, VMD—visual molecular dynamics, J. Mol. Graph. 14 (1996) 33–38.
[10] CHARMM, Chemistry at HARvard Macromolecular Mechanics (CHARMM), http://www.charmm.org/.
[11] B.R. Brooks, C.L. Brooks III, A.D. Mackerell Jr., L. Nilsson, R.J. Petrella, B. Roux, Y. Won, G. Archontis, C. Bartels, S. Boresch, A. Caflisch, L. Caves, Q. Cui, A.R. Dinner, M. Feig, S. Fischer, J. Gao, M. Hodoscek, W. Im, K. Kuczera, T. Lazaridis, J. Ma, V. Ovchinnikov, E. Paci, R.W. Pastor, C.B. Post, J.Z. Pu, M. Schaefer, B. Tidor, R.M. Venable, H.L. Woodcock, X. Wu, W. Yang, D.M. York, M. Karplus, CHARMM: the biomolecular simulation program, J. Comput. Chem. 30 (10, Sp. Iss. SI) (2009) 1545–1614. http://dx.doi.org/10.1002/jcc.21287.
[12] Accelrys, Materials Studio, http://accelrys.com.
[13] W. Chen, J. Fish, A mathematical homogenization perspective of virial stress, Internat. J. Numer. Methods Engrg. 67 (2) (2006) 189–207.
[14] A. Murdoch, A critique of atomistic definitions of the stress tensor, J. Elasticity 88 (2007) 113–140.
[15] A.K. Subramaniyan, C. Sun, Continuum interpretation of virial stress in molecular simulations, Int. J. Solids Struct. 45 (14–15) (2008) 4340–4346.
[16] E.B. Webb, J.A. Zimmerman, S.C. Seel, Reconsideration of continuum thermomechanical quantities in atomic scale simulations, Math. Mech. Solids 13 (3–4) (2008) 221–266.
[17] R. Xu, B. Liu, Investigation on applicability of various stress definitions in atomistic simulation, Acta Mech. Solida Sin. 22 (6) (2009) 644–649.
[18] N.C. Admal, E.B. Tadmor, A unified interpretation of stress in molecular systems, J. Elasticity 100 (2010) 63–143.
[19] R. Maranganti, P. Sharma, Revisiting quantum notions of stress, Proc. R. Soc. A: Math. Phys. Eng. Sci. 466 (2119) (2010) 2097–2116.
[20] J.Z. Yang, X. Wu, X. Li, A generalized Irving–Kirkwood formula for the calculation of stress in molecular dynamics models, J. Chem. Phys. 137 (2012) 134104.
[21] T.W. Sirk, S. Moore, E.F. Brown, Characteristics of thermal conductivity in classical water models, J. Chem. Phys. 138 (6) (2013) 064505.
[22] J. Zhang, S. Ghosh, Molecular dynamics based study and characterization of deformation mechanisms near a crack in a crystalline material, J. Mech. Phys. Solids 61 (8) (2013) 1670–1690.
[23] P.M. Gullett, M.F. Horstemeyer, M.I. Baskes, H. Fang, A deformation gradient tensor and strain tensors for atomistic simulations, Modelling Simul. Mater. Sci. Eng. 16 (1) (2008) 015001.
[24] J.A. Zimmerman, D.J. Bammann, H. Gao, Deformation gradients for continuum mechanical analysis of atomistic simulations, Int. J. Solids Struct. 46 (2) (2009) 238–253.

[25] P.H. Mott, A.S. Argon, U.W. Suter, The atomic strain tensor, J. Comput. Phys. 101 (1) (1992) 140–150.
[26] F. Costanzo, G. Gray, P. Andia, The definitions of effective stress and deformation gradient for use in MD: Hill's macro-homogeneity and the virial theorem, Internat. J. Engrg. Sci. 43 (7) (2005) 533–555.
[27] A. Stukowski, A. Arsenlis, On the elastic–plastic decomposition of crystal deformation at the atomic scale, Modelling Simul. Mater. Sci. Eng. 20 (3) (2012) 035012.
[28] G.J. Tucker, S. Tiwari, J.A. Zimmerman, D.L. McDowell, Investigating the deformation of nanocrystalline copper with microscale kinematic metrics and molecular dynamics, J. Mech. Phys. Solids 60 (3) (2012) 471–486.
[29] K.-I. Saitoh, T. Dan, The method of microscopic strain analysis based on evolution of atomic configuration for the simulation of nanostructured materials, J. Soc. Mater. Sci. Japan 61 (2) (2012) 162–168.
[30] W. Noll, Die herleitung der grundgleichungen der thermomechanik der kontinua aus der statistischen mechanik, Indiana Univ. Math. 4 (5) (1955) 627–646.
[31] K.S. Cheung, S. Yip, Atomic-level stress in an inhomogeneous system, J. Appl. Phys. 70 (10) (1991) 5688–5690.
[32] A. Machová, Stress calculations on the atomistic level, Modelling Simul. Mater. Sci. Eng. 9 (4) (2001) 327.
[33] M. Zhou, D.L. McDowell, Equivalent continuum for dynamically deforming atomistic particle systems, Phil. Mag. A 82 (2002) 2547–2574.
[34] M. Zhou, A new look at the atomic level virial stress: on continuum-molecular system equivalence, Proc. R. Soc. Lond. Ser. A Math. Phys. Eng. Sci. 459 (2037) (2003) 2347–2392.
[35] S. Shen, S.N. Atluri, Atomic-level stress calculation and continuum-molecular system equivalence, CMES Comput. Model. Eng. Sci. 6 (1) (2004) 91–104.
[36] J.A. Zimmerman, E.B. Webb III, J.J. Hoyt, R.E. Jones, P.A. Klein, D.J. Bammann, Calculation of stress in atomistic simulation, Modelling Simul. Mater. Sci. Eng. 12 (4) (2004) S319.
[37] F. Costanzo, G.L. Gray, P.C. Andia, On the notion of average mechanical properties in MD simulation via homogenization, Modelling Simul. Mater. Sci. Eng. 12 (4) (2004) S333.
[38] B. Liu, X. Qiu, How to compute the atomic stress objectively? (2008) arXiv: 0810.0803.
[39] R. Batra, A. Pacheco, Changes in internal stress distributions during yielding of square prismatic gold nano-specimens, Acta Mater. 58 (8) (2010) 3131–3161.
[40] J.A. Zimmerman, R.E. Jones, J.A. Templeton, A material frame approach for evaluating continuum variables in atomistic simulations, J. Comput. Phys. 229 (6) (2010) 2364–2389.
[41] M. Negahban, The Mechanical and Thermodynamical Theory of Plasticity, CRC Press, Taylor & Francis Group, 2012.
[42] Y. Zhou, J.H. Morais-Cabral, A. Kaufman, R. MacKinnon, Chemistry of ion coordination and hydration revealed by a K+ channel-Fab complex at 2.0 angstrom resolution, Nature 414 (6859) (2001) 43–48.
[43] S. Choe, Potassium channel structures, Nat. Rev. Neurosci. 3 (2) (2002) 115–121.
[44] D.A. Doyle, J.M. Cabral, R.A. Pfuetzner, A. Kuo, J.M. Gulbis, S.L. Cohen, B.T. Chait, R. MacKinnon, The structure of the potassium channel: molecular basis of K+ conduction and selectivity, Science 280 (5360) (1998) 69–77.
[45] R. Nashmi, M.G. Fehlings, Mechanisms of axonal dysfunction after spinal cord injury: with an emphasis on the role of voltage-gated potassium channels, Brain Res. Rev. 38 (1–2) (2001) 165–191.
[46] I.M. Williamson, S.J. Alvis, J.M. East, A.G. Lee, The potassium channel KcsA and its interaction with the lipid bilayer, Cell. Mol. Life Sci. CMLS 60 (8) (2003) 1581–1590.